Observation and Simulations of the Backsplash Effects in High-Energy Gamma-Ray Telescopes Containing a Massive Calorimeter

A.A. Moiseev [a,b,*], J. F. Ormes [b], R. C. Hartman [b], T. E. Johnson [b], J. W. Mitchell [b], and D. J. Thompson [b]

[a)] *University Space Research Association, 8501 Forbes Blvd., Seabrook, MD 20706, USA*

[b)] *NASA/ Goddard Space Flight Center, Greenbelt, MD 20771*

Abstract. Beam test and simulation results are presented for a study of the backsplash effects produced in a high-energy gamma-ray detector containing a massive calorimeter. An empirical formula is developed to estimate the probability (per unit area) of backsplash for different calorimeter materials and thicknesses, different incident particle energies, and at different distances from the calorimeter. The results obtained are applied to the design of the Anti-Coincidence Detector (ACD) for the Large Area Telescope (LAT) on the Gamma-ray Large Area Space Telescope (GLAST).

1. Introduction. The common approach to detecting high-energy (≥30 MeV) gamma-rays is a "telescope" consisting of three main parts, the first enabling the conversion of the incident photon into an electron-positron pair and determination of their trajectories (the "tracker"), the second measuring the energy of the photon (the "calorimeter"), and finally an anticoincidence detector covering the aperture to assure neutrality of the incident particle. All astronomical telescopes (SAS-2 [1], COS-B [2], EGRET [3,4], Gamma-1 [5], GLAST [6] and others) are of this basic design. A calorimeter design sufficiently deep to absorb much of the energy of a detected incident photon is used to get reasonable energy resolution on the energy measured that is released in an electromagnetic shower developed in the calorimeter. Most of the charged particles and photons in the shower are traveling along the general direction of the incident photon, but a small fraction of them go backward. The escaping (denoted here as backsplash) radiation can create additional signals in the detectors in front of the calorimeter (e.g. in the tracker). The dominant source of these signals is low attenuation photon backsplash. These photons interact to produce Compton electrons, which then produce signals in particle detectors. For incident energies above several GeV, the number of such secondary particles can be significant.

The purpose of this paper is to explore the special problem of the anti-coincidence detector (hereafter ACD) for the GLAST LAT, a new high energy gamma-ray telescope under development [6]. The ACD is intended to respond to passage of a charged particle; its signal is used as a "veto" to reject such a background event, making possible the detection of the cosmic gamma rays, whose intensity is 4-5 orders of magnitude below that of the charged cosmic rays (protons, helium and other nuclei, electrons).

[*] Corresponding author. Address: NASA/GSFC, code 661, Greenbelt, MD 20771. Tel.: +01-301-286-5581; fax: +01-301-286-1682. E-mail address: moiseev@milkyway.gsfc.nasa.gov

Astroparticle Physics, Volume 22, Issue 3-4, p. 275-283 (2004).

In such a system the backsplash from an incident photon can create ACD signals that mimic veto signals (self-veto effect), thus causing the event to be mistakenly rejected (see Fig. 1). Obviously, this reduces the efficiency of gamma-ray detection, especially at the highest energies. EGRET, the high energy gamma-ray telescope [3,4] on the Compton Gamma Ray Observatory (CGRO), experienced a gamma-ray detection efficiency degradation at an incident photon energy of 10 GeV by a factor of 2 compared to that at 1 GeV, due to the self-veto effect caused by backsplash. The scientific goals of GLAST LAT require it to be capable of detecting photons up to the range of 300-500 GeV (where the instrument will run out of statistics) without significant efficiency degradation due to backsplash. The way to suppress the backsplash effect is to segment the ACD and to consider only that ACD segment in the projected path of the incident photon. This is accomplished through the recognition of the pattern created by photons (and charged particles) and their trajectory reconstruction provided by the tracker. However, a segmented ACD is much more complicated from both mechanical and data acquisition points of view. Thus a deep understanding of the backsplash effect and careful optimization of the ACD are needed.

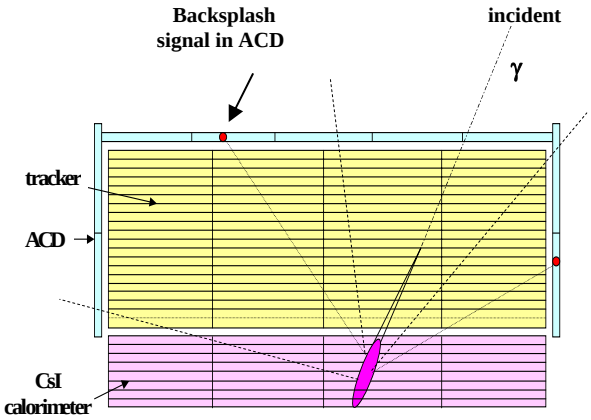

Figure 1. Backsplash in gamma-ray telescope

One approach to the design of such an instrument is the use of computer-generated events to simulate the process of high-energy photon detection by the instrument with a heavy calorimeter, and to optimize the design by minimizing the impact from backsplash. However, we have to take into account that the relevant backsplash from the calorimeter (mainly low-attenuation, several hundred keV photons) causes signals in the ACD via Compton scattering. Because the energy of the incident photon can be several hundred GeV, we must be able to simulate the secondary particles in the shower down in energy by a factor of ~1,000,000. Also, optimization of the design of a complicated mechanical structure by simulations, where the code must be modified many times, can be very time-consuming. Particularly at the initial design level, high precision in the instrument performance prediction seems to be unnecessary.

The goal of the work presented in this paper is to develop a simple, empirical method of estimating the amount of backsplash and to validate a simulation code with experimental data. We conducted a beam experiment to study the backsplash effect quantitatively, and then validated simulations by comparing the experimental results with the simulations. After validation, the simulation code is used for the detailed study of the instrument performance with greater confidence.

2. Measurement of Backsplash.

2.1 Experiment goals and setup. The beam test was performed at the CERN SPS H4 beam line in July 2002. Its task was to measure pulse-height spectra of the backsplash energy deposited in the backsplash detector (hereafter BD), which was placed in front of a simulated calorimeter. This detector served as a prototype of GLAST LAT ACD, made of the same 1 cm thick plastic scintillator, with the same wave-length shifting fiber (WLS) readout. The WLS fiber readout of scintillators has been in use for a number of years in high energy particle physics (see for example [7], [8], [9]). A schematic of the test setup is shown in fig.2. The measurements were done at different distances from the beam axis, with calorimeter simulators of different materials and different thicknesses, and for different BD to calorimeter distances, symbolized by D. A list of beam runs performed, along with simulations runs, is shown in Table 1. The result desired was the probability per unit BD area of a signal caused by backsplash, as a function of distance from the beam axis, calorimeter material and thickness, the separation D, and threshold in the BD. Calorimeters of lead, tin, and iron were used in the test.

E, GeV		10		20		50		100		200		250	
D,cm	Calorimeter	Test	Sim	Test	Sim	Test	Sim	Test	Sim	Test	Sim	Test	Sim
20	Sn, 7.9X_0					√				√	√		
30	Sn, 7.9X_0									√			
45	Sn, 7.9X_0	√		√		√	√	√	√	√	√	√	
	Pb, 7.9X_0			√		√	√	√	√	√	√		
	Pb, 17X_0					√	√	√	√	√	√		
	Pb, 30X_0			√		√	√	√	√	√	√		
	Fe, 7.9X_0					√	√			√	√		
60	Sn, 7.9X_0									√			
80	Sn, 7.9X_0					√				√	√		
Background						√		√		√		√	

Table 1. List of beam tests and simulations runs. D is the distance between the BD and the calorimeter front plane.

Although our ultimate intention was to understand backsplash from photon events, the beam test was done with an electron beam, which is much easier to produce and monitor. The difference between electron-initiated and photon-initiated showers is well understood and reproduced by shower simulation codes. The beam events were selected by the coincidence of three triggering scintillating detectors, two of which were 1cm×1cm size (T1 and T2), and the third one 10cm×10cm (T3), placed directly in front of our detecting system. The BD was composed of 8 plastic scintillating tiles, all 1cm thick. The three closest to the beam were 8cm×24cm and the remaining five 6cm×24cm. Each tile was viewed by one Hamamatsu R647 PMT through wavelength shifting fibers embedded in grooves in the tile. The following calorimeter simulators were available:

9.5 cm thick (~7.9X_0) of tin (Z=50) – a useful simulation of a CsI calorimeter (Cs: Z=55, I: Z=53)

14 cm thick (~7.9X_0) of iron (Z=26)

4.45 cm thick (~7.9X_0) of lead (Z=82)

9.5 cm thick (~17X_0) of lead

17.1 cm thick (~30X_0) of lead

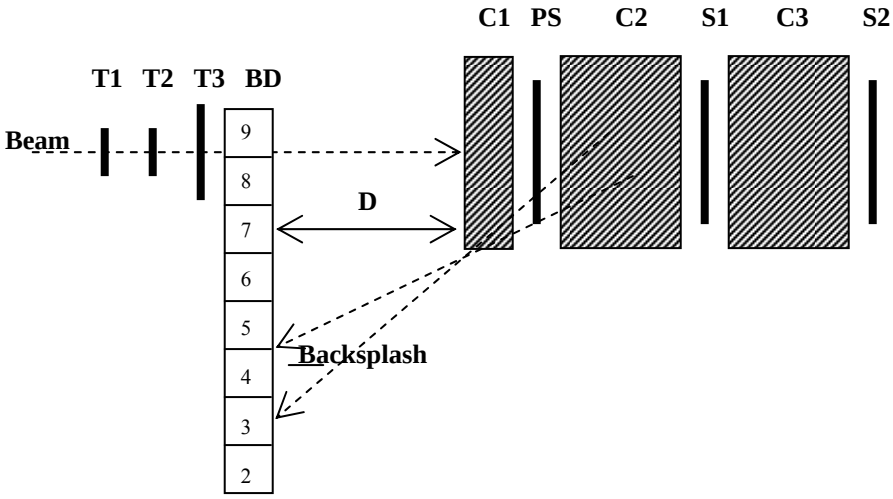

Figure 2. Experimental setup. T1, T2, and T3 – triggering scintillators; BD – tile hodoscope; PS, S1, and S2 – shower detectors; C1, C2, and C3 – calorimeter sections

Three plastic scintillating tiles (shower detectors) are located inside the calorimeter, the first after ~1X_0 of calorimeter depth (PS), the second after 4-5X_0 (S1), and the last in the back of calorimeter (S2). They select the events that had a properly developed cascade in the calorimeter, removing hadron (mostly pion) contamination in the beam.

The BD was placed on a remotely controlled moving table, which permitted adjustment of its position without stopping the beam and entering the beam area.

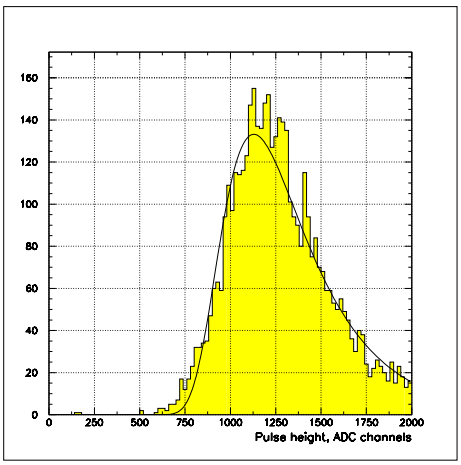

Figure 3. MIP pulse-height spectrum with peak position determined in channel 1129 (pedestal removed) by Landau fitting shown by line

Data acquisition was provided by a CAMAC 2259 peak-sensitive LeCroy ADC, triggered by the coincidence of the three triggering scintillators. Signals digitized were from the three shower detectors and the eight BD tiles. A typical spectrum of signals created in a BD

tile by incident charged particles (here 200 GeV protons, which were used to calibrate the system) is shown in fig. 3.

2.2 Background. In order to measure the pulse-height spectrum in BD tiles from backsplash events, background must be removed. The main background in this experiment is signals produced in BD tiles by bremsstrahlung from beam electrons. The beam setup was such that the electrons were moving through ~20 meters of air between exiting the evacuated beam pipe and entering our experimental setup. Bremsstrahlung photons were created in this region, which make Compton electrons in the BD tiles that are indistinguishable from those created by backsplash photons. In order to be able to remove that background in analysis, the pulse-height spectrum from the BD tiles was recorded with the calorimeter removed from the beam; this was done for several different energies of incident electrons.

2.3 Data Analysis. The raw pulse-heights are converted to units of mean energy deposition in a BD tile using the energy loss of normally incident minimum ionizing singly charged particles (hereafter *mip*). Special runs were performed to do pulse height calibration, with a proton beam incident on each BD tile.

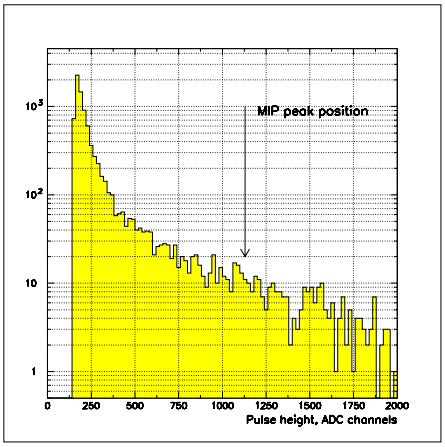

Figure 4. Typical backsplash spectrum with pedestal removed. Arrow shows where the MIP-caused peak would be (as shown in fig.3)

The data analysis procedure was the following:

1. The response of every tile was calibrated with *mips*. The *mip* peak position was determined for each tile by fitting the pulse-height histogram with a Landau distribution.
2. The backsplash spectrum (see Fig. 4) was calibrated in units of energy loss for each tile.
3. For every run the set of events that interacted in the calorimeter was selected by applying selections in the shower detectors PS, S1, and S2. This removed hadron contamination from the events to be analyzed. All further analysis steps were performed on this selected set of events.
4. For every backsplash run, the integral signal distribution in each BD tile was produced by determining the number of events with energy deposition more than 0.1, 0.2, 0.3, 0.4, and 0.5 *mip*.
5. Background runs were treated similarly, and the measured background was subtracted from the corresponding spectrum bin in every run (normally 10-30%). The results were considered to be the backsplash-induced spectra in the BD tiles.

6. In all results presented here (unless stated differently), the backsplash is given as the fraction of events (in percent) in which the signal in the BD was above a given threshold (in units of *mip*). In most figures the backsplash is given for tiles 6, 7, and 8 together, with a total area of 432 cm^2.

2.4 Simulations. A GEANT 3.21 simulation code for all configurations of the experimental setup was written. We mentioned earlier that the signals in the ACD (and in BD) caused by backsplash are created through Compton electrons. GLAST LAT ACD is made of 1 cm thick plastic scintillator, where the mean energy deposition from 1 *mip* at normal incidence is ~2 MeV. In signal processing, we will be dealing with 10%-20% of that signal, or a few hundred keV. Thus signals created by the Compton electrons of this energy would be able to mimic ACD veto signals from *mips,* and consequently the simulations have to track secondary particles in the shower down to this "cutoff" energy. This is a key parameter in such simulations, and requires tracking of many generations of secondary particles and thus very significant computing time and computer memory. In our simulations, the kinetic energy cutoff was set to 100 keV.

The output data was organized in a manner very similar to that for the beam test, and analysis on this data was performed in the same way as on the beam test data. This approach allowed us to minimize the approximations in comparing the beam test and simulations results.

3. Results.

3.1. Angular distribution of backsplash. As the first step of the analysis, the angular dependence of backsplash was determined. This is important because of the necessity to check the validity of application of the results to other sizes of detectors (here, tiles). The angle at which the tile was seen from the calorimeter axis was measured between the beam axis and the line connecting the center of the calorimeter face and the corresponding tile center. The results are given in fig. 5 for five thresholds used in the analysis. Each data point represents a particular tile. Hereafter the backsplash is given as the fraction of events (in percent) when the signal in a BD tile was above a given threshold. The area of each tile was 144 cm^2 (backsplash in the larger area tiles 2, 3, and 4 was scaled to the same area). These data in fig. 5 are for a 200 GeV

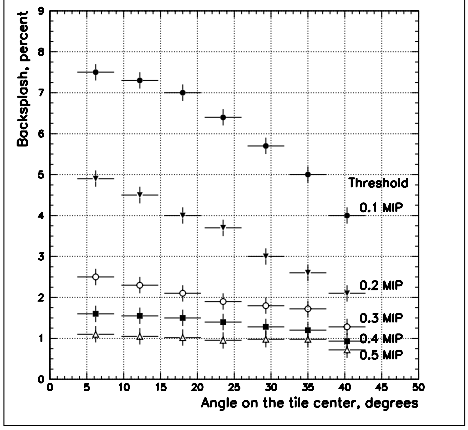

Figure 5. Angular distribution of backsplash for different thresholds. Data are for 200 GeV beam with the tin calorimeter placed at 45cm from BD

electron beam, taken with the tin calorimeter placed 45 cm from the BD plane.

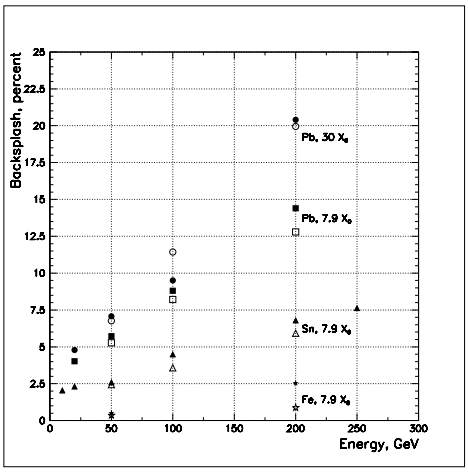

Figure 6. Backsplash (in percent) energy dependence for calorimeter placed at 45cm from BD and threshold 0.3 MIP. Filled points are for test results, open points are for simulations. Circles - $30X_0$ lead calorimeter, squares - $7.9X_0$ lead, triangles - $7.9X_0$ tin, and stars - $7.9X_0$ iron

3.2. Energy dependence of backsplash. The measured backsplash energy dependence for different calorimeter materials is shown in fig. 6. This is given by filled points for tiles 6, 7, and 8 together (total area 432 cm^2), placed at 45 cm from the calorimeter face. The threshold used in this figure was 0.3 *mip*. The difference in the backsplash intensity between the iron and lead calorimeters, with the same thickness in radiation lengths, is quite dramatic. It is also seen that the backsplash is significantly lower for the $7.9X_0$ lead calorimeter than that for $30X_0$ lead, especially at higher incident energy. This is due to the fact that the shower is not fully developed and contained in the thinner calorimeter at higher energy. Simulation results are also shown in fig. 6 by open points. The attempt to build the energy and threshold part of an empirical formula is demonstrated in fig. 7, where the energy fitting for the tin calorimeter is given. The energy part of dependence is fitted by $E^{0.5}$, and the threshold dependence is fitted by $e^{-threshold\,/\,0.19mip}$. An average fitting precision of ~10% is achieved. It must be noted that this fitting is appropriate only for this material (Sn, or similar Z) and thickness of BD, appropriate for the GLAST ACD.

3.3 Backsplash distance dependence. Backsplash was measured for five different distances between the BD and the calorimeter, using the tin calorimeter as the best imitator for a CsI calorimeter. Fig. 8 shows the backsplash distance dependence for the $7.9X_0$ thick tin calorimeter. The data points are given by filled circles, and simulations results – by open circles, for energies 50 GeV and 200 GeV. The lines are the fittings by [55/(D+15)] where D is the distance between BD and calorimeter front face in cm. For better fitting, the value 15, which is related to the position of the shower maximum in the calorimeter, should probably be logarithmically energy dependent to reflect the shower development energy dependence.

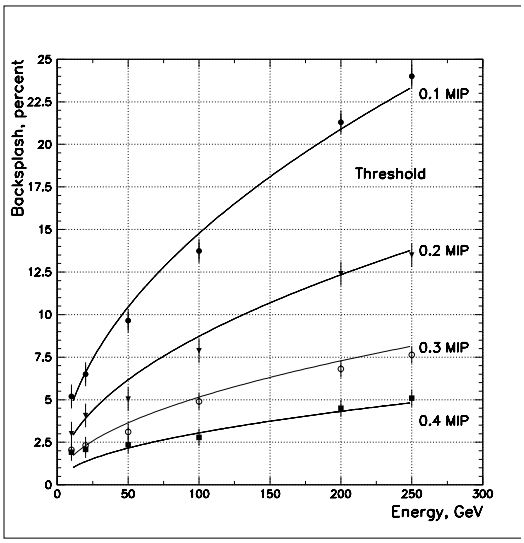

Figure 7. Fitting of backsplash energy dependence for $7.9X_0$ tin calorimeter at 45cm from BD. Points represent test data, and lines – fitting.

Combining all the effects we arrive at our empirical formula:

$$P_{backsplash} = 2.5 \times \exp\left(-\frac{E_{thr}}{0.19}\right) \times \frac{A}{432} \times \left(\frac{55}{D+15}\right)^2 \times \sqrt{E} \qquad (1)$$

where $P_{backsplash}$ is the percentage probability of detecting backsplash, with threshold E_{thr} (measured in *mip*), in a tile of area A (in cm^2) separated by D cm from the front face of calorimeter, at an incident electron (photon) energy E (in GeV). This formula is valid for a calorimeter of 8-9X_0 thick CsI (or material of similar average Z). The simulations and measurements agree within approximately 10%, which is acceptable for the present purposes.

Formula (1) will suffice for our efforts to build an empirical formula for use in LAT ACD and its application will be discussed below in Section 4. Here we extend this formula to other calorimeter thicknesses and materials.

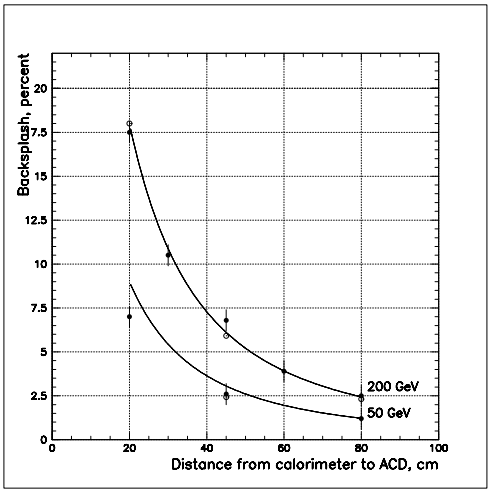

Figure 8. Backsplash distance dependence for 7.9X_0 tin calorimeter for two energies. Filled circles are for test data, open circles - simulations. Lines are for fitting by formula (1)

3.4 Calorimeter thickness dependence.

Measurements were performed for lead calorimeters of three thicknesses (7.9X_0, 17X_0, and 30X_0) and four incident energies (20, 50, 100, and 200 GeV). The results are shown in fig. 9. The increase in backsplash with increasing thickness from 7.9X_0 to 17X_0 and the saturation of the backsplash for 30X_0 at these energies are due to the shower containment effect. (Shower maximum in lead is at ~8.5X_0 for 50 GeV, at ~9X_0 for 100 GeV, and at ~9.7X_0 for 200 GeV). Based on these results, we can slightly extend our formula for larger calorimeter thicknesses up to 13-14X_0. A correction factor F to be applied to the backsplash value in our formula (1) can be expressed as

$$F = 1 + 0.07 \times (T-7.9),$$

where the calorimeter thickness in radiation lengths is T, so the corrected value of backsplash probability P_{corr} will be $P_{corr} = P_{backsplash} \times F$

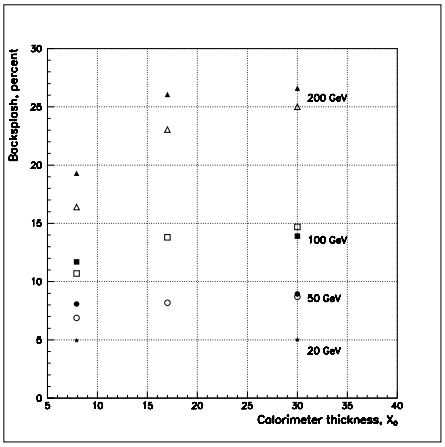

Figure 9. Backsplash thickness dependence for lead calorimeter placed at 45cm from BD. Filled points are for test data, and open points - simulations. Triangles - 200 GeV, squares - 100 GeV, circles - 50GeV, and stars - 20 GeV

3.5 Calorimeter material dependence. It was noted in our earlier simulations that backsplash intensity is strongly affected by the Z of the calo-

rimeter material. Electromagnetic calorimeters of the same thickness in radiation lengths create less backsplash if they are made of lower Z (larger X_0 in g/cm^2) material. This can be explained by the fact that the backsplash consists mainly of soft photons whose attenuation is determined by grammage, not radiation lengths. Fig. 10 shows the results of our test along with the simulations. These results demonstrate that, when the backsplash is an issue in the design of a high-energy electromagnetic calorimeter, it can be significantly reduced by optimizing the calorimeter material, but at the expense of increased calorimeter size and mass. We found that if the calorimeters have the same depth in radiation lengths, but are made of different materials, the backsplash from them is proportional to $\approx Z^{1.95} e^{-0.04T}$, where Z is the calorimeter material atomic number and T is its depth in g/cm^2. These expressions can be used for quantitative consideration of the calorimeter material.

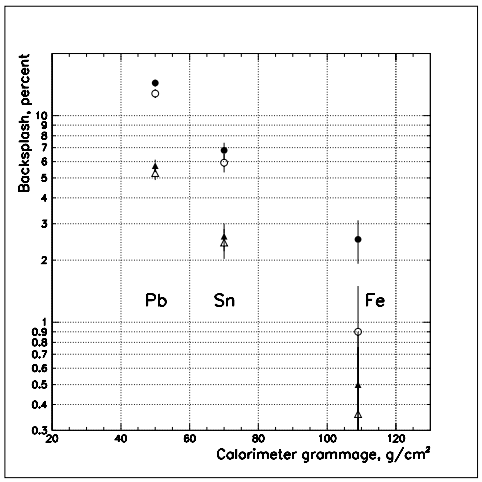

Figure 10. Backsplash for different calorimeter materials. Filled points are test data, and open points - simulations. Circles are for 200 GeV, and triangles are for 50 GeV. Results are given for threshold of 0.3MIP, with calorimeters placed at 45cm from BD

4. Predictions for GLAST ACD and Conclusions

We used the results obtained to design the GLAST ACD segmentation. The ACD was designed to the requirement that the backsplash-caused self-veto should remove not more than 20% of otherwise accepted gamma-ray events at 300 GeV, with a threshold in ACD set to 0.3 *mip*. This requirement must be reconciled with the ACD charged particle detection efficiency requirement (to be >0.9997 over the entire ACD area), because higher detection efficiency can be achieved by reducing signal threshold, but that increases backsplash-caused self-veto. The backsplash prediction for GLAST ACD, based on our tests, is shown in fig. 11. It can be seen that at 300 GeV, self-veto due to backsplash is to be expected to be ~7% in the single ACD tile crossed by the incident gamma-ray, with the threshold set to 0.3 *mip*.

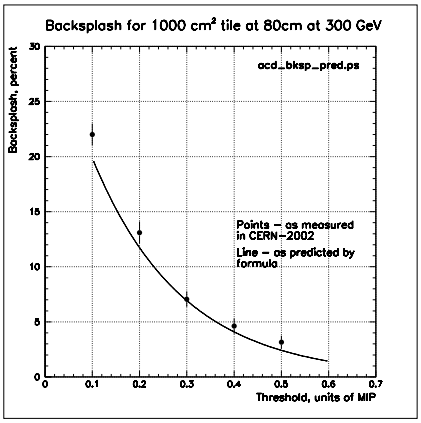

Figure 11. Predictions for LAT ACD for 1000 cm^2 tile at 80cm from calorimeter. Filled circles are data points as measured in test, scaled to the LAT ACD tile area. Line as predicted by formula (1).

The empirical formula (1) can be used in high-energy particle detector design where backsplash is an issue, avoiding complicated and time-consuming Monte Carlo simulations. The utilization of this formula is limited to the detectors similar to ACD (BD), 1 cm thick plastic scintillators. Further study is required to extend these results to

other materials such as Si. The results obtained also can be used in calorimeter optimization, for example in the proposed missions for detection of high-energy cosmic rays, where the backsplash is also an undesirable effect.

5. Acknowledgements

This work could not have been completed without the extremely valuable help of Deneen Ferro and Bill Daniels (detector fabrication and refurbishing) and Norm Dobson (data acquisition system). The authors are very grateful to Prof. Tune Kamae and Tsunefumi Mizuno for their help in conducting the beam test and to Steven Ritz and Robert Streitmatter for very valuable discussions and recommendations in the preparation stage. Special thanks go to CERN SPS personnel, who were extremely helpful in all aspects of the beam test.

6. References

[1] C.E. Fichtel et al., Astrophys. J. 198 (1975) 163

[2] K. Bennett, Nuclear Physics B (Proc. Suppl) 14B (1990) 23

[3] D.J. Thompson et al., Astrophys. J. Supp. 86 (1993) 629

[4] C.E. Fichtel et al., Astronomy & Astrophysics Suppl. Ser. 97 (1993) 13

[5] V.V. Akimov et al., Astronomicheskiy Zhurnal, 17 (1991) 6, 501

[6] N. Gehrels, and P. Michelson, Astroparticle Phys. 11 (1999) 277

[7] G. F. Knoll, Radiation Detection and Measurement, John Wiley & Sons, New York, 1989

[8] M. G. Albrow et al., Nuclear Instruments and Methods A256 (1987) 23

[9] P. L. Hink et al., SPIE 1549 (1991) 193

Figure Captions.

Fig.1 Backsplash in gamma-ray telescope

Fig.2 Experimental setup. T1, T2, and T3 – triggering scintillators; BD – tile hodoscope; PS, S1, and S2 – shower detectors; C1, C2, and C3 – calorimeter sections

Fig.3 MIP pulse-height spectrum with peak position determined in channel 1129 (pedestal removed) by Landau fitting shown by line

Fig.4 Typical backsplash spectrum with pedestal removed. Arrow shows where the MIP-caused peak would be (as shown in fig.3)

Fig.5 Angular distribution of backsplash for different thresholds. Data are for 200 GeV beam with the tin calorimeter placed at 45 cm from BD

Fig.6 Backsplash (in percent) energy dependence for calorimeter placed at 45 cm from BD and threshold 0.3 MIP. Filled points are for test results, open points are for simulations. Circles – $30X_0$ lead calorimeter, squares – $7.9X_0$ lead, triangles – $7.9X_0$ tin, and stars – $7.9X_0$ iron

Fig.7 Fitting of backsplash energy dependence for $7.9X_0$ tin calorimeter at 45 cm from BD. Points represent test data, and lines – fitting.

Fig.8 Backsplash distance dependence for $7.9X_0$ tin calorimeter for two energies. Filled circles are for test data, open circles – simulations. Lines are for fitting by formula (1)

Fig.9 Backsplash thickness dependence for lead calorimeter placed at 45 cm from BD. Filled points are for test data, and open points – simulations. Triangles – 200 GeV, squares – 100 GeV, circles – 50 GeV, and stars – 20 GeV

Fig.10 Backsplash for different calorimeter materials. Filled points are test data, and open points – simulations. Circles are for 200 GeV, and triangles are for 50 GeV. Results are given for threshold of 0.3 MIP, with calorimeters placed at 45 cm from BD

Fig.11 Predictions for LAT ACD for 1000 cm^2 tile at 80 cm from calorimeter. Filled circles are data points as measured in test, scaled to the LAT ACD tile area. Line as predicted by formula (1).